

# Thermokinetic instabilities for ammonia-hydrogen mixtures in a Jet Stirred Flow Reactor

Maria Virginia Manna<sup>a,b,\*</sup>, Pino Sabia<sup>b,\*</sup>, Raffaele Ragucci<sup>b</sup>, Mara de Joannon<sup>b</sup>

<sup>a</sup>Università degli Studi di Napoli Federico II

<sup>b</sup>Istituto di Scienze e Tecnologie per l'Energia e la Mobilità Sostenibili (STEMS-CNR)

[mariavirginia.manna@unina.it](mailto:mariavirginia.manna@unina.it)

The oxidation of ammonia and the interaction between ammonia and hydrogen chemistry have been extensively studied at high temperatures for traditional flames, while no experimental evidences have been provided for conditions relevant to MILD (Moderate or Intensive Low-oxygen Dilution) combustion. The high dilution levels and the relatively low working temperatures have been proven to promote thermo-kinetic instabilities, with detrimental effects on pollutant emissions and process efficiency.

Given this background, first, this work reports on an experimental characterization of NH<sub>3</sub>-O<sub>2</sub>-N<sub>2</sub> instabilities in a Jet Stirred Flow Reactor. Oxidation regimes were consequently reassessed in T<sub>in</sub>- $\phi$  (preheating temperature T<sub>in</sub>, and equivalence ratio  $\phi$ ) maps.

Second, the effect of H<sub>2</sub> as a fuel "enhancer" on the identified NH<sub>3</sub>-O<sub>2</sub>-N<sub>2</sub> oxidation regimes was numerically investigated, parametrically changing the H<sub>2</sub> concentration itself. Results suggested that small concentrations of H<sub>2</sub> strongly enhance the system reactivity and tighten the T<sub>in</sub>- $\phi$  windows where instabilities occur.

Kinetic analyses suggested that H<sub>2</sub> strongly interacts with NH<sub>2</sub> radicals, enhancing the overall NH<sub>3</sub> oxidation chemistry, thus, suppresses the instabilities.

## 1. Introduction

The transition of the energy scenario towards no-carbon economy is becoming mandatory within 2050, because of fossil fuels depletion and CO<sub>2</sub> strict emissions regulations, while worldwide energy demand is increasing (World Energy Outlook, 2019). Within this panorama, the green and blue ammonia (Ye et al., 2017) has received a lot of attention as no-carbon fuel and also as hydrogen vector because of its high hydrogen density with respect to other molecules (Aziz et al., 2018). Ammonia benefits from already available storage and delivery infrastructures, as well as some well-established production technologies and plants (Valera-Medina et al., 2019). While these advantages make ammonia worth of a careful evaluation on its potentials as an energy vector, its physical/chemical properties (high auto-ignition temperatures, low laminar flame speed, relatively low calorific power) represent an hindrance to its practical use both in stationary plants and transportation systems. Different strategies have been proposed to overcome these drawbacks. Blending ammonia with hydrogen could allow to stabilize the oxidation process, without giving up a carbon-free energy production system (Li et al., 2014). On the other hand, the higher heating value of hydrogen leads to high working temperatures, thus promoting the thermal-NO<sub>x</sub> formation. Therefore, it becomes necessary to keep the temperature lower than the threshold values for NO<sub>x</sub> production. Due to the high dilution levels and relatively low temperatures with respect to traditional combustion processes, MILD combustion (Cavaliere and de Joannon, 2004) could be a promising solution to oxidize NH<sub>3</sub>-H<sub>2</sub> mixtures, without exceeding NO<sub>x</sub> emission limits. MILD process has been also proven to allow the combustion of pure ammonia (Sorrentino et al., 2019).

Nonetheless, the use of low temperature combustion modes, under diluted conditions, may force the system to work with low-intermediate temperature oxidation chemistry that, coupled with heat exchange phenomena, could promote the onset of thermo-kinetic instabilities, with negative effects on the energy efficiency of the process (Chinnick et al., 1987) and pollutants formation. Recently, Manna et al. (2021) have proven dynamic

behaviours can occur for NH<sub>3</sub>-O<sub>2</sub>-N<sub>2</sub> mixtures in a Jet Stirred Flow Reactor (JSFR) at environmental pressure. Given this background, authors' experimental results were re-organized with respect to system external parameters, i.e. T<sub>in</sub> (mixture preheating temperature) and φ (mixture equivalence ratio), and reassumed in T<sub>in</sub>- φ maps of behaviour, to better highlight the operating conditions that lead to process instability.

Therefore, the work was devoted to numerically investigate the plausible use of H<sub>2</sub>, as a fuel "enhancer", to stabilize the dynamic behaviours, experimentally detected, for NH<sub>3</sub>-O<sub>2</sub>-N<sub>2</sub> mixtures, and consequently improve the overall efficiency of the oxidation process. This approach to the problem consists in a preliminary analysis, preceding the realization of dedicated experimental tests.

The code PSR of Chemkin-PRO and a detailed kinetic mechanism, able to predict the main features of the different oxidation regimes on the basis of previous investigations, were used.

The numerical study was performed by parametrically changing the H<sub>2</sub> content in the reference mixtures while re-drawing the T<sub>in</sub>- φ maps of behaviours. Given the success of the chosen strategy, further detailed kinetic analyses were carried out to understand the interaction between the H<sub>2</sub> and NH<sub>3</sub> oxidation chemistry, under the explored operative conditions.

## 2. Methodology

The experimental tests were run in a quartz Jet Stirred Flow Reactor (JSFR). The JSFR approaches the behaviour of a Perfectly Stirred Reactor (PSR). It allows to analyse the effect of the system external parameters (pressure, pre-heating temperature, residence time, dilution level and equivalence ratio) on the reactivity of the mixture. The reactor used for this experimental campaign is a quartz spherical reactor of 113 cm<sup>3</sup>. It is located within two ceramic fiber semi-cylindrical electrically-heated ovens. The temperature within the reactor is measured by an unshielded thermocouple type R (Pt-Pt 13% Rh wire, 40 μm bead size) with an accuracy of ±2 K with a fast response time (less than 20 ms). In addition, a National Instruments module capable of acquiring 95 samples per second for each channel was installed. This configuration allow to analyse also oscillatory oxidation regimes in time. To monitor the process homogeneity, two further thermocouples (type N) are located respectively within the exit tube and the premixing chamber.

A detailed description of the reactor is reported elsewhere (Manna et al., 2021).

The experiments were performed for NH<sub>3</sub>/O<sub>2</sub>/N<sub>2</sub> mixtures diluted at d=86% as a function of mixture inlet temperature (T<sub>in</sub>) and equivalence ratio (φ), at a fixed residence time (τ=0.21 s) under atmospheric pressure (p=1.2 atm). The equivalence ratio (φ) was defined based on the reaction 4NH<sub>3</sub>+3O<sub>2</sub>=2N<sub>2</sub>+6H<sub>2</sub>O, according to the following Eq (1):

$$\phi = \frac{(NH_3/O_2)}{(NH_3/O_2)_{stoich}} = \frac{3}{4}(NH_3/O_2). \quad (1)$$

The experimental tests were repeated at least three times and also verified in different days under the same operating conditions.

In the cases of H<sub>2</sub>-NH<sub>3</sub>/O<sub>2</sub>/N<sub>2</sub> systems, the equivalence ratio was defined based on the reactions 4NH<sub>3</sub>+3O<sub>2</sub>=2N<sub>2</sub>+6H<sub>2</sub>O and 2H<sub>2</sub>+O<sub>2</sub>=2H<sub>2</sub>O, according to the following Eq (2):

$$\phi_{H/O} = \frac{(3NH_3 + 2H_2)/2O_2}{((3NH_3 + 2H_2)/2O_2)_{stoich}} \quad (2)$$

According to the given definition, the O<sub>2</sub> concentration changes as a function of the total H moles of the mixture. The effect of H<sub>2</sub> was evaluated by changing the parameter R, defined as the mole fraction of H<sub>2</sub> on the total moles of fuels, according to the Eq (3):

$$R = \frac{H_2}{NH_3 + H_2} \quad (3)$$

In particular, R was changed from 0.05 to 0.20 with a step of 0.05.

The system was modeled as "non-adiabatic" with a global heat transfer coefficient equal to 3.5×10<sup>-3</sup> cal/cm<sup>2</sup> s K, estimated according to the procedure reported in (Manna et al., 2020). The experimental results were simulated with the "transient" equations of PSR code of Chemkin PRO package, in order to analyze the system behaviour in time.

Several updated kinetic mechanisms were used. For the sake of brevity, herein the results and chemical kinetic analyses are reported for the Zhang mechanism (Zhang et al., 2017).

### 3. Results

#### 3.1 Experimental results

The oxidation of  $\text{NH}_3$  as a function of the equivalence ratio ( $\phi=0.4-1.4$ ) and preheating temperature ( $T_{in}=1250-1300\text{K}$ ) was experimentally investigated by measuring the species concentrations and recording the temporal reactor temperature profiles ( $T_r$ ). Several typologies of  $T_r$  profiles were recognized, thus defining different associated combustion regimes:

- *No Reactivity*: no reaction occurs and  $T_r$  increment is lower than 5K.
- *Low Temperature (LT)*: it is characterized by low reactant conversion (lower than 30%) and moderate temperature increment (lower than 30K).
- *Dynamic Regime (DR)*: the evolution of the system passes through damped temperature oscillations in time; the amplitude of the oscillations decreases with the elapsed time while the frequency increases.
- *High Temperature (HT)*: it is characterized by high temperature increment (higher than 30K) and almost complete reactants conversion.

The system behavior, in terms of combustion regimes, is reported on the map in the  $\phi$ - $T_{in}$  plane (Figure 1a). For each  $\phi$  and  $T_{in}<1230$  K, no reactivity was observed (grey area). For  $T_{in}>1230$  K, different regimes can be recognized depending on  $\phi$ . In particular, the LT area (blue area) is wider for ultra-lean conditions and it becomes smaller as the equivalence ratio increases, whereas the HT one (red area) is larger for fuel ultra-rich conditions. The DR (dotted area) was observed for fuel-lean conditions within the temperature range  $T_{in}=1260-1290$  K.

Typical  $T_r$  profiles for each oxidation regimes are reported in Figure 1b. In particular, such temperature profiles were recorded at  $\phi=0.9$  and  $T_{in}=1250, 1270, 1290$  K but they represent qualitatively the overall system behavior within the associated combustion regimes.

For the LT regime (blue line),  $T_r$  increases slowly in time from the initial value to the stationary condition (blue line). For the DR regime (grey line)  $T_r$  increases slowly up to 1310 K, then damped temperature oscillations occur and they extinguish at  $T_r=1320$  K. Subsequently,  $T_r$  increases to the stationary value.

Finally, for the HT regime (red line), the temperature increases monotonically in time and reaches the stationary value faster than the  $T_r$  profiles in the LT and DR regimes.

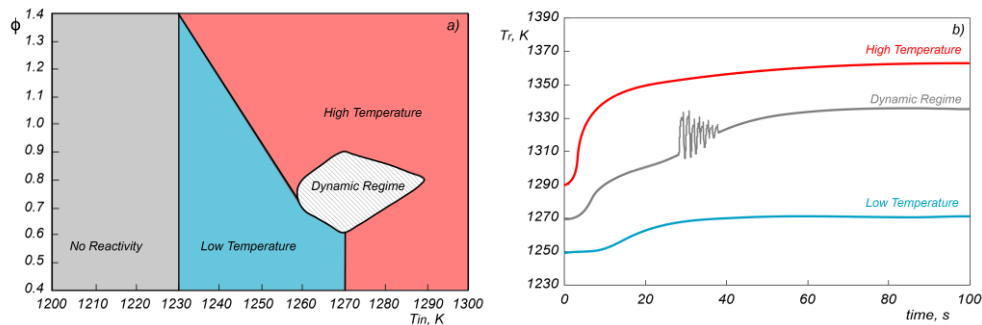


Figure 1. Experimental Map of combustion behaviors and characteristic  $T_r$  profiles for  $\text{NH}_3/\text{O}_2/\text{N}_2$  mixtures diluted at 86% in  $\text{N}_2$ , at  $p=1.2$  atm and  $\tau=0.21$  s.

#### 3.2 Numerical results

The effect of  $\text{H}_2$  on  $\text{NH}_3$  combustion regime was investigated by numerical simulations using the detailed kinetic mechanism by Zhang et al. (2017). The parameter  $R$  was varied from 0 (reference case) up to 0.15 with a step of 0.05. The reference case also allows to value the capability of the considered kinetic model to predict the experimental data reported in Figure 1.

Based on the previous definitions, it was possible to outline the numerical maps of behaviors in the  $\phi$ - $T_{in}$  plane for each considered  $R$  value (Figure 2). It must be highlighted that the numerical DR areas identify periodic temperature oscillations in time, while the experimental ones refer to damped temperature oscillations. In fact, the numerical study did not reveal the occurrence of damped instabilities under the explored operating conditions.

The map at  $R=0$  shows that no reaction occurs for  $T_{in}<1240$  K. For  $\phi=1.2-1.4$  the "No Reactivity" area expands to higher temperatures (up to 1260 K). The LT regime is predicted for  $T_{in}=1240-1270$  K. These numerical results partially agree with the experimental data, even though the experimental evidences suggest slightly higher reactivity under ultra-rich conditions. The "Dynamic Regime" is observed for fuel-lean conditions within  $T_{in}=1270-$

1280 K and the dotted area tightens around  $\phi=0.9$  for higher temperatures. The HT regime is predicted for  $T_{in}>1270$  K, outside the DR area.

As the  $H_2$  is added to the mixture, the system reactivity increases. In fact, at  $R=0.05$  the “No Reactivity” area disappears. The LT area is shifted towards lower  $T_{in}$  as  $R$  increases and it completely disappears at  $R=0.15$ . Also the DR region is moved toward lower temperatures as  $R$  increases and its shape and extension strongly change with  $R$ . For instance, at  $T_{in}=1250$  K and  $R=0.05$ , oscillations were predicted at  $\phi=1.0$  while at  $R=0.1$  and  $R=0.15$ , the temperature instabilities occur only under fuel-lean conditions. In additions, the DR area becomes narrower as  $R$  increases and it disappears at  $R=0.2$  (not reported in the Figure 2).

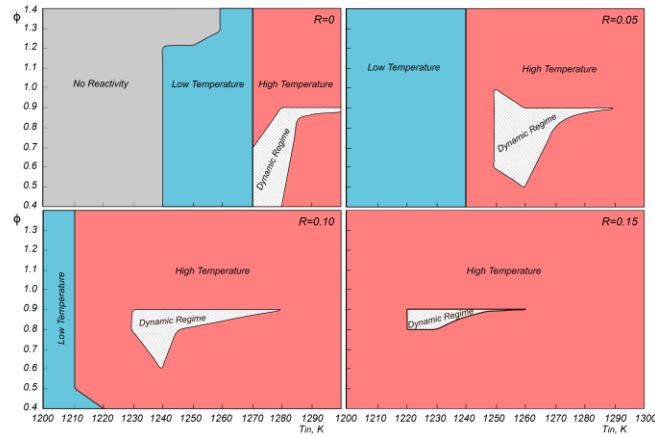


Figure 2. Numerical maps of combustion behaviors for  $NH_3-H_2/O_2/N_2$  mixtures for  $R=0, 0.05, 0.10, 0.15$ , diluted at 86% in  $N_2$ , at  $p=1.2$  atm and  $\tau=0.21$  s.

### 3.3 Reaction Rate analysis

In order to further investigate the effect of hydrogen on  $NH_3$  oxidation chemistry, several kinetic analyses were performed. In particular, the fuel-lean mixture at  $\phi=0.9$  was considered for this study, because it exhibits all the identified combustion behaviors as a function of the temperature and  $R$ .

The main oxidation pathways are reported as flux diagrams for both LT and HT regimes, at steady conditions. For each diagram, ammonia and nitrogen species are reported in black, while  $H_2$  and radicals from  $H_2/O_2$  mechanism are reported in red. The same color code is used for arrows, that identify the reactions the species are involved in. Arrow thickness is proportional to the RR value, reported in the round brackets, and the overall order of magnitude of the RRs is reported in the legend.

Figure 3 shows the controlling chemistry for  $NH_3$  oxidation without  $H_2$  (reference case,  $R=0$ ).

For both LT and HT regimes,  $NH_3$  is mainly dehydrogenated to  $NH_2$  through the reaction  $NH_3+OH=NH_2+H_2O$ . Subsequently, depending on the system temperature,  $NH_2$  can be converted to  $N_2$  following different routes.

For the LT regime, the controlling pathway can be summarized as follow:  $NH_3 \rightarrow NH_2 \rightarrow H_2NO \rightarrow HNO \rightarrow NO \rightarrow NNH \rightarrow N_2$ . The OH radicals, that are involved in the  $NH_3$  oxidation, are produced directly from the reaction  $NH_3+O=NH_2+OH$  or from the typical  $H_2/O_2$  high-temperature branching mechanism, namely  $H+O_2=OH+O$ . The H radicals, that feed this reaction, derive from NNH decomposition reaction ( $NNH=N_2+H$ ), thus the branching mechanism at low temperature is strictly dependent on the nitrogen species chemistry. On the other hand, the HT oxidation can be described by the following pathways:  $NH_3 \rightarrow NH_2 \rightarrow NH \rightarrow N_2O \rightarrow N_2$  and  $NH_3 \rightarrow NH_2 \rightarrow HNO \rightarrow NO \rightarrow NNH \rightarrow N_2$ . The OH production at higher temperature passes through the reaction  $H+O_2=OH+O$  and it is boosted by the  $H_2O$  decomposition reaction ( $H_2O+O=OH+OH$ ). The H radicals are produced through NNH decomposition and  $H_2$  direct oxidation ( $H_2+OH=H+H_2O$ ).

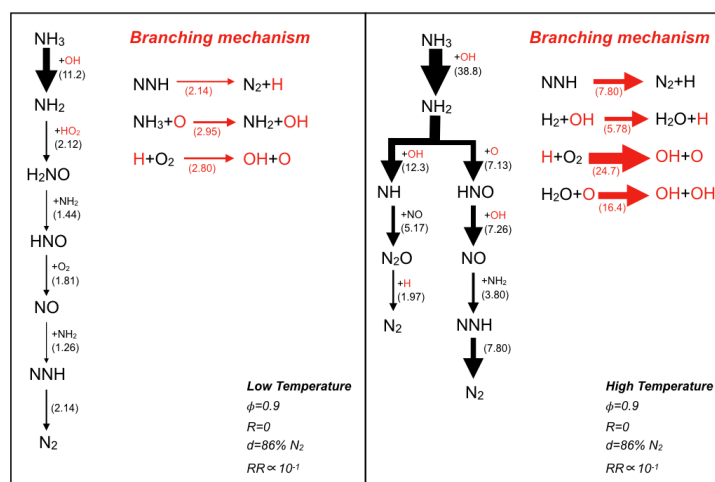


Figure 3. Flux diagram at  $R=0$  and  $\phi=0.9$  for LT and HT regimes.

Figure 4 reports the flux diagrams for LT and HT regimes for the  $\text{NH}_3\text{-H}_2/\text{O}_2/\text{N}_2$  mixture in case of  $R=0.10$ . This condition represents a compromise to discuss the enhancing effect of  $\text{H}_2$  on  $\text{NH}_3$  combustion, because for lower  $\text{H}_2$  concentration,  $\text{NH}_3$  chemistry still controls the oxidation process while for higher  $\text{H}_2$  content, the  $\text{H}_2$  oxidation reactions are predominant (for instance, in case of  $R=0.15$ , the LT regime is shifted to temperature lower than 1200 K).

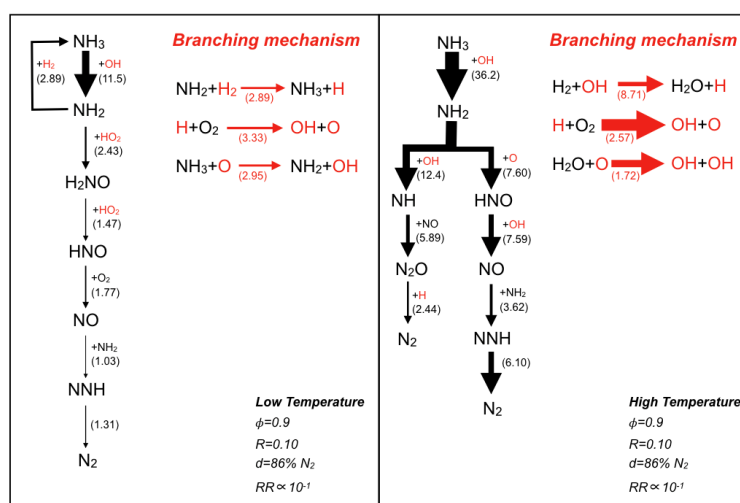


Figure 4. Flux diagram at  $R=0.10$  and  $\phi=0.9$  for LT and HT regimes.

For the LT, the  $\text{NH}_3$  oxidation can be described by the same pathway identified at  $R=0$  ( $\text{NH}_3 \rightarrow \text{NH}_2 \rightarrow \text{H}_2\text{NO} \rightarrow \text{HNO} \rightarrow \text{NO} \rightarrow \text{NNH} \rightarrow \text{N}_2$ ). The major difference due to the presence of  $\text{H}_2$  is represented by the reaction between  $\text{NH}_2$  radical and  $\text{H}_2$  ( $\text{NH}_2 + \text{H}_2 = \text{NH}_3 + \text{H}$ ). Even though this reaction reconverts  $\text{NH}_2$  to  $\text{NH}_3$ , it strongly boosts the production of H radicals that feed the branching mechanism through the reaction  $\text{H} + \text{O}_2 = \text{OH} + \text{O}$ , thus increasing the system reactivity. In fact, in this case,  $\text{NNH}$  decomposition is not the primary source of H radicals.

Similarly, for the HT it is possible to recognize the same reaction pathways for the  $\text{NH}_3$  oxidation, namely  $\text{NH}_3 \rightarrow \text{NH}_2 \rightarrow \text{NH} \rightarrow \text{N}_2\text{O} \rightarrow \text{N}_2$  and  $\text{NH}_3 \rightarrow \text{NH}_2 \rightarrow \text{HNO} \rightarrow \text{NO} \rightarrow \text{NNH} \rightarrow \text{N}_2$ . The reaction between  $\text{NH}_2$  and  $\text{H}_2$  becomes slower as the temperature increases and the main H source is represented by  $\text{H}_2$  direct oxidation ( $\text{H}_2 + \text{OH} = \text{H} + \text{H}_2\text{O}$ ).

To sum up,  $\text{H}_2$  promotes the H production through the interaction with the  $\text{NH}_2$  radical ( $\text{NH}_2 + \text{H}_2 = \text{NH}_3 + \text{H}$ ) for low temperatures and through its direct oxidation ( $\text{H}_2 + \text{OH} = \text{H} + \text{H}_2\text{O}$ ) for higher ones. As a result, the concentration

of OH radicals in the radical pool strongly increases via the reaction  $\text{H} + \text{O}_2 = \text{OH} + \text{O}$ , thus enhancing the overall system reactivity.

#### 4. Conclusions

The experimental results reported in this paper show the existence of different oxidation regimes for highly diluted  $\text{NH}_3\text{-O}_2$  mixtures as a function of the equivalence ratio and preheating temperature. No Reactivity, Low and High Temperature combustion regimes are described. The transition from the LT to the HT can occur through damped temperature oscillations in time, in particular under fuel-lean conditions, thus defining a Dynamic Regime.

Numerical simulations were able to predict the establishment of different oxidation regimes for the reference system, even though some discrepancies occur with respect to the location of the several regimes in the  $T_{in}\text{-}\phi$  map.

Following, the effect of  $\text{H}_2$  on the map of combustion behaviours is numerically studied, for the same operating conditions, parametrically changing the  $\text{H}_2$  content in the reference mixture.

The numerical results show that hydrogen strongly enhances the mixtures reactivity, also for small  $\text{H}_2$  concentrations. For instance, the No Reactivity area disappears as  $\text{H}_2$  is added to the mixture and the LT and DR regions shift to lower temperatures as  $\text{H}_2$  concentration increases. In addition, the DR area becomes even narrower increasing the  $\text{H}_2$  mole fraction.

Flux diagrams analyses were performed to identify plausible kinetic controlling routes for the establishment of the oxidation regimes and to understand the interaction between  $\text{NH}_3$  and  $\text{H}_2$  oxidation chemistry. In case of neat ammonia, the LT oxidation is controlled by the slow  $\text{NH}_3$  oxidation reactions, that can be summarized by the following pathway:  $\text{NH}_3 \rightarrow \text{NH}_2 \rightarrow \text{H}_2\text{NO} \rightarrow \text{HNO} \rightarrow \text{NO} \rightarrow \text{NNH} \rightarrow \text{N}_2$ . The production of H radicals, that promote the branching mechanism, is strictly connected to this pathway, since the main source of H radical is the reaction  $\text{NNH} = \text{N}_2 + \text{H}$ . For high temperatures, the ammonia oxidation pathway changes to a faster kinetic mechanism and the H radicals production is boosted by the  $\text{H}_2$  direct oxidation.

When hydrogen is added to the mixture, for lower temperatures, it interacts with  $\text{NH}_2$  radicals through the reaction  $\text{NH}_2 + \text{H}_2 = \text{NH}_3 + \text{H}$ . Despite this reaction reconverts  $\text{NH}_2$  to  $\text{NH}_3$ , it enhances the H radical production, thus increasing the overall system reactivity.

#### References

- Aziz M., Juangsa F.B., Triawan F., Nandiyanto A.B., Abdullah A.G., 2018, Integrated Nitrogen Production and Conversion of Hydrogen to Ammonia, *Chemical Engineering Transactions*, 70, 571-576.
- Chinnick K., Gibson C., Griffiths J.F., Kordylewski W., 1986, Isothermal interpretations of oscillatory ignition during hydrogen oxidation in an open system. Analytical predictions and experimental measurements of periodicity, *Proceedings of the Royal Society of London. A. Mathematical and Physical Sciences*, 405, 117-128.
- Cavaliere A., de Joannon M., *Mild Combustion*, 2004, *Progress in Energy and Combustion Science*, 30, 329-366.
- Manna M.V., Sabia P., Ragucci R., de Joannon M., 2021, Ammonia oxidation regimes and transitional behaviours in a Jet Stirred Flow Reactor, *Combustion and Flame*, 228, 388-400.
- Li J., Huang H., Kobayashi N., He Z., Nagai Y., 2014, Study on using hydrogen and ammonia as fuels: Combustion characteristics and  $\text{NO}_x$  formation. *International journal of energy research*, 38, 1214-1223.
- Manna M.V., Sabia P., Ragucci R., de Joannon M., 2020, Oxidation and pyrolysis of ammonia mixtures in model reactors. *Fuel*, 264, 116768.
- Sorrentino G., Sabia P., Bozza P., Ragucci R., de Joannon M., 2019, Low- $\text{NO}_x$  conversion of pure ammonia in a cyclonic burner under locally diluted and preheated conditions, *Applied Energy*, 254, 1-7.
- Valera-Medina A., Xiao H., Owen-Jones M., David W.I.F., Bowen P.J., 2018, Ammonia for power, *Progress in Energy and Combustion Science*, 69, 63-102.
- World Energy Outlook 2019, The gold standard of energy analysis <<https://www.iea.org/weo2018>> accessed 05.01.2021.
- Ye L., Nayak-Luke R., Banares-Alcantara R., Tsang E., 2017, Reaction: "green" ammonia production. *Chem*, 3, 712-714.
- Zamfirescu C., Dincer I., 2009, Ammonia as a green fuel and hydrogen source for vehicular applications. *Fuel processing technology*, 90, 729-737.
- Zhang Y., Mathieu O., Petersen E.L., Bourque G., Curran H.J., 2017, Assessing the predictions of a  $\text{NO}_x$  kinetic mechanism on recent hydrogen and syngas experimental data. *Combustion and Flame*, 182, 122-141.